Lafayette College Switched LF RFID Reader: Version 0.95

Jon W. Wallace

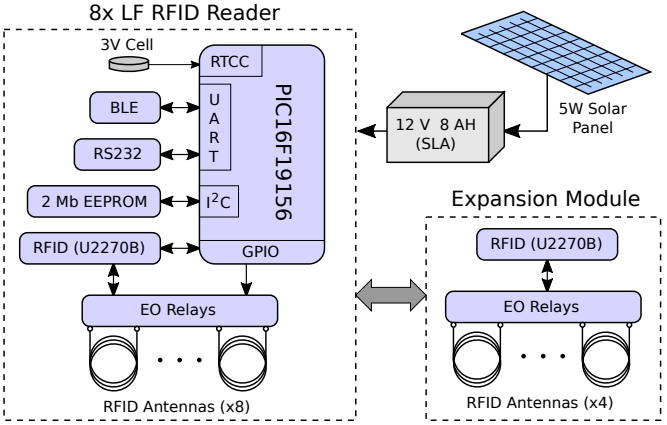

Fig. 1. Block diagram of hardware components of the switched-antenna RFID system.

I. Introduction

This report provides an overview of the switched-antenna low-frequency (LF) radio-frequency identification (RFID) reader that has been developed for ornithology studies at Lafayette College. The RFID reader currently supports scanning of eight RFID antennas, expandable to 12 antennas with an external module. The reader has been designed for low-power solar operation, typically consuming less than 0.5 W. The design supports a Bluetooth Low Energy (BLE) interface to allow remote control and wireless data download. The design may be freely used by others according to the MIT License.

II. System Design Details

This appendix describes the hardware and software components that were developed to characterize the switched-antenna RFID concept, as well as collect data for a useful application.

A. Hardware Components

Fig. 1 depicts a block diagram of the switched-antenna RFID system that we have developed. The purpose of this document is to give an overview of the system architecture. Complete schematics, layouts, and firmware are available online [1]. The PIC16F19156 microcontroller (PIC) has been chosen as the heart of the system, mainly due to its very low power consumption and on-board real-time calendar and clock (RTCC) capability. The main system components are described in detail below:

1) Universal Asynchronous Receiver Transmitter (UART): Transfer of data and commands is accomplished using a single universal asynchronous transmitter receiver (UART) on the PIC. Having wireless connectivity through this interface is desirable for many reasons, but foremost to ensure system robustness. Since the sensors are deployed for long periods of time in potentially adverse conditions, they must be sealed in waterproof containers. Frequent opening of these enclosures to download sensor data can lead to faults as the electronics and lead wires are disturbed. Under normal operation, wireless connectivity can eliminate this type of failure.

Bluetooth low energy (BLE) was chosen for wireless transfer due to much lower power requirements than standard Bluetooth or WiFi. Our sensors currently leverage the Adafruit nRF51822 BLE module, which can be directly connected to the universal asynchronous receiver transmitter (UART) of the PIC. For testing, it is desirable to allow a cable connection to the UART, which is supported by a standard RS232 interface on the sensor that is selectable with a jumper.

2) EEPROM: Low-power non-volatile storage is accomplished using a 2-Mb (256-kbyte) electrically erasable programmable read-only memory (EEPROM) part (M24M02). Reserving 1k of space for system configuration information, approximately 23700 tag read events can be stored (11 bytes per event).

3) RFID Transceiver: A simplified schematic of the RFID transceiver and switch array is depicted in Fig. 2. The RFID transceiver contains a differential source that pumps the RLC circuit formed by a capacitor, resistor, and the antenna (inductor) at the resonant frequency near 125 kHz. The current in the antenna coil generates a magnetic field that powers the RFID tag, which in turn emits a 125-kHz signal that amplitude modulates the field and antenna coil current. The modulating waveform is recovered by rectifying, filtering, and amplifying the coil signal. Normally, the transceiver wires COILA and COILB would be attached to a single antenna, but in our system they are attached to a switch array (described below).

The Atmel U2270B was chosen as the RFID transceiver due to good read range and previous familiarity with this part. Future designs will likely need to migrate to a more modern part like the EM Microelectronic EM4095. This single-coil transceiver is powered directly from the 12-V rail, allowing higher coil voltages (and larger read range) than similar 5-V transceivers.

4) Switch Array: The switch array is depicted in the non-shaded portion of Fig. 2, whose purpose is to selectively connect one out of N antennas to the COILA/COILB differential pair. A simple parallel switch arrangement has been found to work effectively, where one side of each antenna

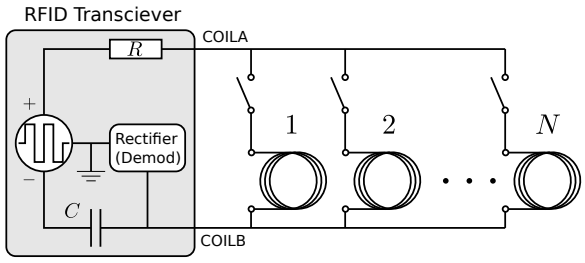

Fig. 2. Schematic diagram showing interconnection of the RFID transceiver with the parallel switch array.

connects to a common point (COILB) and the other antenna terminal is selectively connected through a switch to COILA. The antennas are scanned in a sequential fashion with one antenna active at a time.

Since a resonating LF RFID antenna presents a fairly high peak voltage, care is required in selecting appropriate switch elements. We have chosen the IXYS CPC1017N solid state relay, providing a blocking voltage of 60 V, and a low turn-on current of 1 mA. These relays are optically coupled, providing good isolation between the high-voltage antenna signals and the low-voltage microcontroller. Finally, they are inexpensive, with a unit price of around USD 0.50.

Parasitic capacitance of the switch in the "off" state is the main degradation to read range performance. The CPC1017N presents approximately 7 pF "off" capacitance, which is quite low compared to other options we researched. Note that better isolation could be achieved by switching both COILA and COILB lines, but this comes at the cost of more switch elements and higher current consumption.

5) Expansion Module: Our target application requires 12 antennas with separate 8- and 4-element subarrays. We have found that the simple parallel switch arrangement with more than 8 antennas significantly degrades performance due to non-ideal switch isolation. Further, long lead wires on RFID antennas can lead to reliability and signal integrity issues. We have overcome these problems by developing a simple expansion board carrying an additional RFID transceiver and four switch elements. Power, switch control, and digital RFID signals connect from the main reader to the expansion module over an inexpensive CAT5 Ethernet cable. RFID signals for the two separate readers are multiplexed in the digital domain, precluding any problems due to cable length or switch isolation. Note that the PIC only enables a single antenna (either on the main board or the expansion board) at a time, avoiding interference of the two RFID modules.

6) Clocks: Although not depicted in the diagram, two key clocks are used in the digital system. A precision, but very low-power 32.768-kHz clock is always present, which is used for system timing events, such as the RTCC. During active operation, the internal PIC clock runs at a modest 8 MHz to conserve power.

7) Power: The system is powered using a 12-V 8-Ah sealed lead acid (SLA) battery, which is kept charged using a 5-W solar panel. A 3-V lithium coin cell powers the RTCC from a dedicated PIC pin, ensuring that date and time information is not lost. Care has been taken to minimize power consumption

TABLE I
SYSTEM CURRENT CONSUMPTION

Console: PIC On, RFID Off		Scanning: PIC On, RFID On		Sleep: PIC Sleep, RFID Off	
12 V	1.8 mA	12 V	28 mA	12 V	0.1 mA
3 V	0.6 μA	3 V	0.6 μA	3 V	0.1 μA

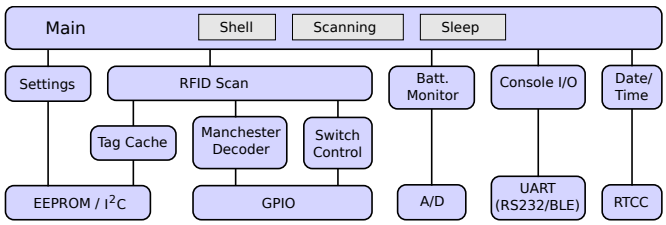

Fig. 3. Firmware components of the switched-antenna RFID system.

of the overall system, and table I lists measured current draw on the 12-V (main battery) and 3-V (coin cell) supplies for the three system modes. In *console* mode, the PIC is active and accepts user commands, but the RFID chip is off. In *scanning* mode, assuming 100% read duty cycle, the RFID chip is active and the EEPROM is being written. Finally, in the *sleep* mode, all possible hardware resources are powered off and the PIC sleeps. For the 12-V 8-Ah battery, the system can run in scanning mode for 12 days on battery power alone. Average current draw by the Bluetooth module is approximately 5 mA when not connected to a remote device, and 10 mA when connected.

When the battery voltage drops below a set threshold (we use 11.0 V), the board enters the ultra-low-power sleep mode, which remains in effect until the voltage rises again to a safe level. The purpose of this sleep mode is to avoid complete drain of the battery, which dramatically shortens its lifespan. Additionally, the sleep mode provides reliability in low voltage (brown-out) conditions, since the microcontroller is always kept in a known, controlled state.

The 5-W solar panel is more than sufficient to keep the battery charged over long periods of time, because even at 100% read duty cycle, power consumption is only $12\ \mathrm{V} \times (28\ \mathrm{mA} + 5\ \mathrm{mA}) = 0.40\ \mathrm{W}$. Experience has shown that the system indeed runs without any loss-of-power events, even during frequent cloudy days in eastern Pennsylvania.

B. Firmware Components

Fig. 3 presents a diagram showing system firmware components. For minimal code size, the firmware uses a single-threaded, bare metal (no operating system) approach. After initialization, a main program loop executes in one of three modes. In the *console* mode, the user is presented with a basic shell over the UART that allows commands to be executed and system settings to be changed. In the *scanning* mode, the system sequentially excites the RFID antennas and records tags encountered in the tag cache and EEPROM. The scanning mode can be set to start automatically from the console mode after a timeout, and it can be terminated using a command from the UART. The *sleep* mode is entered when the battery

voltage drops below a set threshold and is exited when battery voltage exceeds a different set threshold.

Although most of the components in Fig. 3 are self explanatory, a few design choices should be highlighted:

1) Tag Cache: To conserve memory and minimize data transfer times, identified RFID tags are stored in a *tag cache*, where the number of elements (cache lines) and cache timeout can be controlled with a console setting. The cache is fully associative, and each cache line stores the RFID code, a timestamp, and an antenna hit count array.

The cache operates as follows. When a tag is seen, the cache is searched for a matching entry. If it is not found, the first unused line is filled, or the line having the oldest entry is logged in EEPROM and overwritten in the cache. At this first sighting, the timestamp (time and date) is also stored, and the antenna hit count for the active antenna index is set to 1. If a tag is found in the cache, only the antenna hit count is incremented for the active antenna index on that cache line. Each time the RFID scan process switches antennas, the cache is checked for entries that are older than the timeout. Those entries are logged in EEPROM and set to be unused, thus ensuring that tag information is permanently logged periodically.

The savings in EEPROM memory using the cache can be dramatic. For example, assuming a cache size of at least 12 elements, the timeout set to 5 minutes, and the same tags being constantly present on all 12 antennas, the EEPROM will fill up at a rate of 12 entries per 5 minutes, meaning the EEPROM will be full after about 6.9 days. If no cache is used, and the antenna scanning period is 1 s, the EEPROM will fill at 12 entries per second, becoming full after only 33 minutes.

2) Manchester Decoder: The manchester decoder was developed from scratch using an application note associated with the U2270B [2]. Read robustness was further optimized by toggling GPIO outputs on the PIC for key events and comparing the timing of those events with the RFID digital output signal with an oscilloscope. Since at the 8-MHz clock rate, instruction time can be comparable to event timings, it is likely that timing values would need to be adjusted for different clock rates or a different microcontroller.

3) EEPROM Driver: EEPROM is very low power, has centuries of expected data retention, and is byte addressable. However, the maximum number of repeated write cycles to a single location is limited (4 million for the M24M02 part). Since it is hoped to deploy these RFID sensors for several years without needing replacement, ensuring the longevity of the EEPROM is a key concern. The most frequently written location of the EEPROM in our design is a pointer that indicates the end of the RFID data log. Although the pointer could just be stored in RAM and written to EEPROM occasionally, tag information could be lost in a power failure. Therefore, for data robustness the pointer is written for each log entry write to the EEPROM.

In our initial design, a single location was used for the end-of-log pointer, and assuming writing 12 entries every 5 minutes, the maximum number of write cycles would be exceeded after 3.2 years. This was changed to use a "scratch pad" approach, where a 512-byte circular buffer in EEPROM is sequentially written with the incrementing pointer. For a 2-byte pointer and the assumptions above, this extends the EEPROM lifespan to approximately 820 years.

4) Bluetooth Low Energy (BLE): As described previously, wireless connectivity to the sensors is highly desirable for our application. One firmware consideration is the speed of the BLE interface (Adafruit nRF51822 module) which defaults to 9600 baud. We have found that error free operation is also possible at 19200 baud, but that higher baud rates lead to errors, likely due to lack of UART handshaking in our design. The current design sends data as ASCII hexadecimal values, and for a full EEPROM (23700 entries), this requires approximately 4 minutes to download. This time could be reduced by sending binary data and by implementing handshaking. However, in our application we download sensor data on a monthly basis, and download times are typically 30 seconds or less. Data robustness is important in our design, and the firmware implements a 16-bit cyclic redundancy check (CRC16-CCITT) to ensure data integrity during download.

Since BLE is a fairly recent standard, BLE UART support is not commonly found in existing smartphones, tablets, or laptops. Adafruit provides the BlueFruit LE Connect App for Android to communicate with their BLE modules. We have slightly modified this app to provide a log download feature that can receive the RFID sensor log data, check integrity with the CRC, expand the data into human readable form, and store the result in a text file.

III. Antenna Design

Two types of antennas have been used with the RFID sensor, as depicted in Fig. 4. The antennas were constructed by hand winding the wire onto a cylindrical core and then wrapping the coil tightly with electrical tape. For antennas that were likely to be immersed in water, the antennas were covered in PlastiDip, providing a waterproof coating. This turned out to be critical for antennas placed on the ground, where unprotected antennas could easily become filled with water.

Proper inductance of each antenna was checked by connecting the antenna in series with a 1.2-nF capacitor to a sine-wave generator and finding the frequency giving maximum voltage across the antenna. We found that antenna inductance could be increased by as much as 0.1 mH by making a twisted pair out of the antenna lead wires with a drill. This approach avoids having to disassemble, modify, and reassemble the antennas to obtain a target inductance. Although the target inductance of an isolated antenna is 1.35 mH for 125 kHz resonance, the switch array increases the effective antenna inductance, and this effect increases with array size. Therefore, lower target inductances were used.

The antenna in Fig. 4(a) has a target inductance of 1.21 mH, constructed with 69 turns of AWG24 wire, wound on a core of radius 10 cm. The purpose of this relatively large antenna is to cover areas on the ground where birds are likely for forage for food. The antenna in Fig. 4(b) has a target inductance of 1.28 mH, consisting of 140 turns of AWG24 wire, wound on a core of radius 4 cm. This smaller antenna was designed to be attached near perches on a bird feeder.

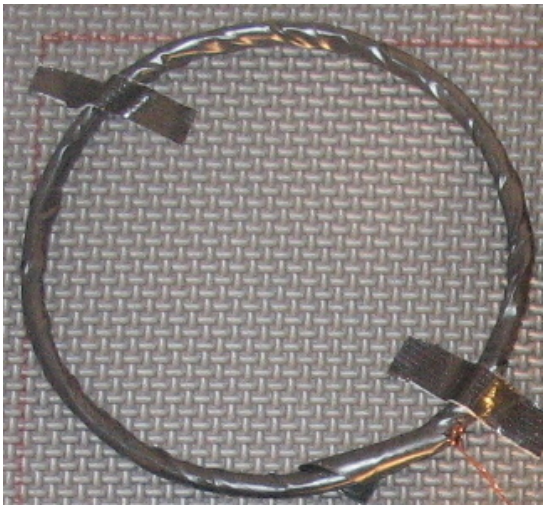

(a)

(b)

Fig. 4. Two types of antennas used with the switched RFID reader.

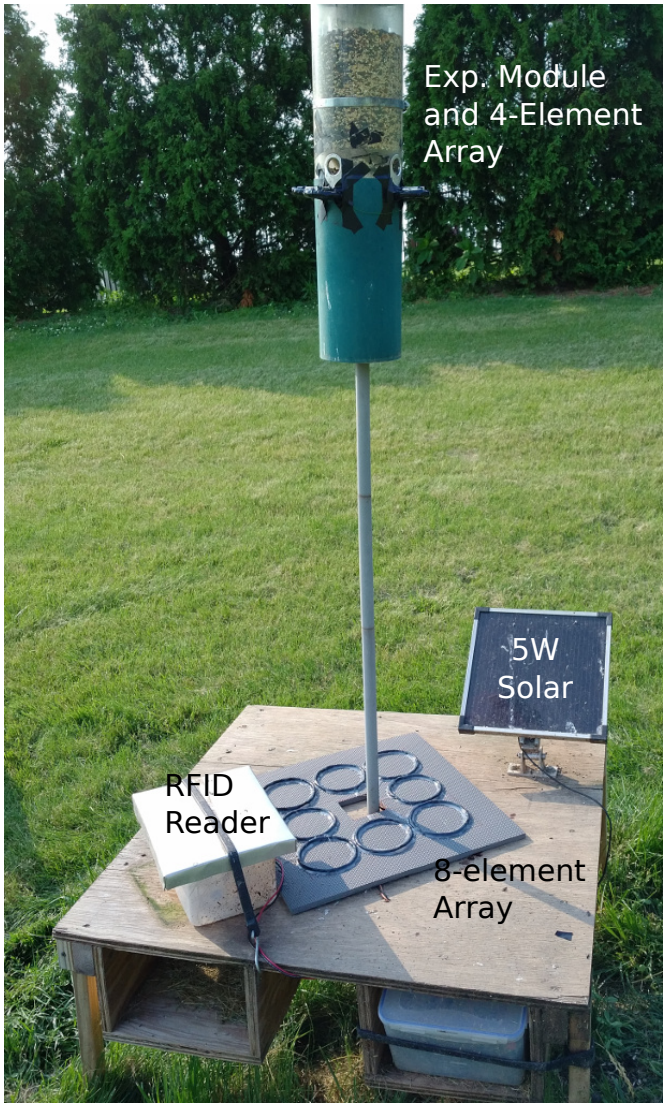

Fig. 5. RFID monitored feeder station employing the prototype prototype reader.

IV. Typical Deployment

Fig. 5 shows a typical deployment of the switched RFID reader. The RFID sensor and expansion module monitor a total of 12 antennas at the feeder station, with four antennas placed on the bird feeder (one at each perch) and eight placed on a mat on the ground. Four 4-cm antennas on the feeder are placed directly beneath the perches using the 3D-printed hanger depicted in Fig. 6, and this placement has been justified through read reliability measurements. It is worth noting that the perches on the feeder are aluminum, which appears to have little effect on the RFID antennas mounted to them. Eight 10-cm antennas on the ground mat are arranged in a square 3×3 array with the center element missing, thus providing a space for the feeder pole. The mat is made from foam floor tile material, where the antennas have been sewn to the foam with nylon fishing line. Our early designs used silicone caulk and hot-melt glue for attachment, which did not last in the field.

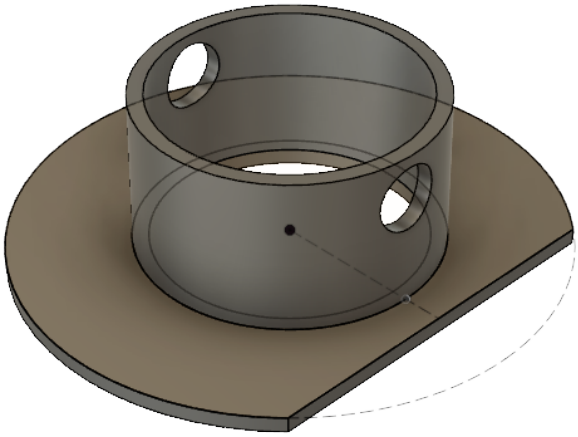

Fig. 6. 3D printed hanger used to hold the 4-cm RFID antennas to the bird feeder perches.

V. Conclusion

This document has provided a high-level description of the hardware and software components of the Lafayette College

switched RFID reader. Detailed schematics, layout, etc., may be found online [1].

REFERENCES

[1] http://jonwallace.org/.

[2] "Electronic immobilizers for the automotive industry," TEMIC Semiconductors, Tech. Rep. ANT019, 1996.